Impact of Compressed Sensing With Quantization on UWB Receivers With Multipath Channel Estimation

Osama Ullah Khan, Shao-Yuan Chen, David D. Wentzloff, and Wayne E. Stark, *Fellow, IEEE*

***Abstract*—This paper explores the application of compressive sensing (CS) for ultra wide band (UWB) communication. Channel estimation is an important aspect for any communication system and especially for UWB systems in order to appropriately collect the energy from the multipath channel. UWB generally requires a high sampling rate since the bandwidth is large. Channel estimation using CS is studied along with its impact on reducing the sampling rate for an ADC to reduce power. Practical issues regarding the effect of quantization on channel estimation are addressed and a hardware implementation for CS based on the Walsh–Hadamard transform (WHT) allowing sub-Nyquist sampling is proposed. To separate the effect of channel estimation with CS, the performance of the sub-Nyquist ADC is studied in a noiseless and multipath free channel and design decisions are discussed. Comparison with the Nyquist ADC shows that using the sub-Nyquist ADC reduce power by a factor of about 6×. For the proposed hardware, two receiver architectures based on matched filtering and filtering in the compressed domain (so-called "smashed filtering") are studied. It is found that with a perfect channel smashed filtering performs better than matched filtering. Finally the effect of channel estimation on the proposed hardware is studied along with two different recovery algorithms namely basis pursuit and matching pursuit.**

***Index Terms*—Channel estimation, compressive sensing (CS), sub-Nyquist ADC, Walsh–Hadamard transform (WHT).**

I. Introduction

WIRELESS communication systems and wireless computation are becoming as ubiquitous as microelectronics are today. Due to the form factor limitation, the battery size on these portable/mobile electronics is limited and, therefore, there is an increased interest in energy-efficient circuit design and techniques. One way to reduce the required transmitted energy for each bit is to employ wide-bandwidth signals, such as ultra wide band signals (UWB). However, wide-bandwidth signals generally require significant energy for high rate sampling and the associated signal processing algorithms to process the received signals. However, in certain cases where the signals are sparse it may be possible to reduce the sampling rate using an approach called compressed sensing.

Compressed sensing (CS) theory states that given a signal is sparse in one domain (e.g., a pulse in the time domain); it can be sampled randomly in an orthogonal domain (e.g., the frequency domain) at a rate less than that suggested by the Nyquist sampling theorem. The sparse signal can then be recovered with high probability from these "compressed" samples, but with an error proportional to the compression rate, by using a suitable recovery algorithm (e.g., L1 minimization).

The signal of interest here is a baseband ultra wide band (UWB) pulse with a width on the order of a nanosecond which is sparse in the time domain. The Nyquist sampling rate for a UWB pulse requires ADC sampling at a frequency greater than a GHz, which usually results in prohibitively large power consumption in the ADC. This power can be a significant fraction of the total power consumption of the entire system. In [1]–[3] the power consumption for a 6-bit ADC with a sampling rate in the range of 1.2–1.6 GHz is greater than 150 mW, which might be excessive for certain applications. Sampling the UWB signal below Nyquist rate (sub-Nyquist) may lead to a low power alternative solution. Since our goal is not recovering the signal directly but recovering the data being transmitted by the signal, a lower sampling rate would be possible.

Channel estimation is a critical issue in a communication system. This is especially true for a UWB system since the transmitted signal energy, which is small to begin with, is split into many multipath channel components. It is crucial to accurately estimate the channel multipath delay spread to collect and combine the energy in various multipath components. Unfortunately, the components with low amplitude are difficult to estimate. The transmitted reference (TR) approach in [4] reduces the sampling rate by correlating the received signal with a template derived from the reference signal and then sampled at the frame rate to determine the signal. However, TR suffers significant performance degradation, particularly at low signal-to-noise ratio (SNR) due to the fact that the reference signal is noisy.

CS was introduced in [5] to address the high sampling rate issue in multipath channel estimation. In [5], each entry of the projection matrix is a random variable with Gaussian distribution. The receiver in [5] only performs matched filtering with random Gaussian distributed project signals but no smashed filtering to detect the information bits. Because the correlation with random Gaussian signals is difficult to implement, we consider an alternative approach which is to use Hadamard signals instead of random signals. In addition, [5] did not consider the important aspects of quantization of signals. Other papers have also considered compressed sensing for channel estimation. In [6], an overview of the application of CS to pilot-aided channel estimation is given. In [7], a channel estimation strategy using compressive sampling matching pursuit (CoSaMP) algorithm is described. The algorithm combines the greedy algorithm and convex programming. In [8], a method to estimate the channel

Manuscript received March 02, 2012; revised August 06, 2012; accepted September 17, 2012. Date of publication November 15, 2012; date of current version December 05, 2012. This work is supported by the Signal Processing, Information Technology Program of the National Science Foundation under Award CIF-0910765. This paper was recommended by Guest Editor R. Rovatti.

The authors are with the Department of Electrical Engineering and Computer Science, University of Michigan, Ann Arbor, Michigan 48109-2122 (e-mail: oukhan@umich.edu).

Color versions of one or more of the figures in this paper are available online at http://ieeexplore.ieee.org.

Digital Object Identifier 10.1109/JETCAS.2012.2222220

using smooth L0 (SL) algorithm is presented. The performance of this algorithm is slightly better than CoSaMP. The authors in the last two papers use different recovery algorithms from what we consider. None of these schemes considered the effect of quantization which is essential for circuit implementation and energy consumption analysis.

In this paper, we apply CS theory [9], [10] for low power circuit design and its application to wireless communication. We propose using the Hadamard transform as a measurement matrix, as opposed to a Guassian matrix for CS considering also the difficulty of implementation. We further investigate the effect of quantization of the received signal and the application of matched filtering in the compressed domain (smashed filtering [11]) instead of applying a matched filter in the time domain. In this way, the same circuit structure can be used to estimate the channel for pilot bits and detect the transmitted information bits. We also propose a practical hardware implementation for computing the Hadamard projections (HP) and provided the design criteria for selecting the number of compressed measurement K and the resolution of a sub-Nyquist ADC. Further, the power saving for the sub-Nyquist ADC is evaluated as compared to the Nyquist ADC with the proposed Walsh Hadamard Transform (WHT) front-end. Finally, We evaluate the performance of the different receivers using matching pursuit (MP) [12] and spectral projected-gradient (SPGL1) [13] recovery algorithms to obtain the channel template.

The rest of this paper is organized as follows. Section II discusses channel estimation and compares it with different receiver architectures. In Section III, keeping the practical constraints in mind, we propose hardware for CS which is amenable to circuit implementation. Section IV discusses some fundamental questions related to the proposed hardware and Section V presents simulation results with and without channel estimation. Section VI concludes the paper.

II. Channel Estimation

A. UWB Transmitted Signal

We consider a simple communication system that uses nanosecond pulses $p(t)$. Assume we transmit one pulse in one frame with interval T_f between two consecutive pulses and one bit consists of N_f frames. The transmitted signal with duration $T_b = N_f T_f$ can be described as

$$s_(t) = \sum_k b(k) \sum_{j=0}^{N_f-1} p(t - jT_f - kT_b) \tag{1}$$

where $b(k) \in \{-1, 1\}$ is the k-th binary bit that modulates the amplitude and $p(t)$ has duration $T_p \ll T_f$.

B. Channel Model

We consider the following multipath channel impulse response as our model:

$$h(t) = \sum_{\ell=0}^{L-1} \alpha_\ell \delta(t - \tau_\ell) \tag{2}$$

where $\delta(t)$ is Dirac delta function, τ_ℓ and α_ℓ are the path delay and path gain of the ℓ-th path of multipath channel, respectively. The number of paths in the channel is denoted by L and τ_{L-1} is the maximum delay spread of the channel. We assume that $h(t)$ remains static for N_s bits and assume $T_f \geq \tau_{L-1} + T_p$ so that there is no intersymbol interference. Fig. 2 shows a realization of a particular channel impulse response based on our model. For this channel and a frame duration with $T_f = 40$ ns, there would be no ISI.

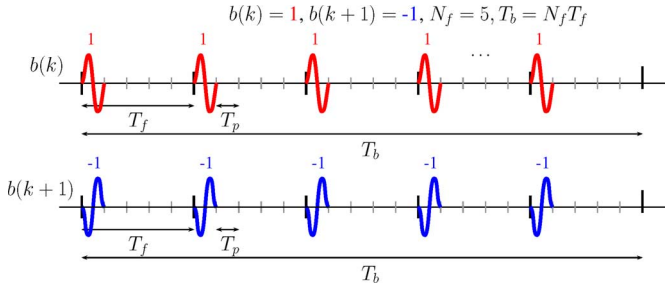

Fig. 1. Transmitting pulses $p(t)$.

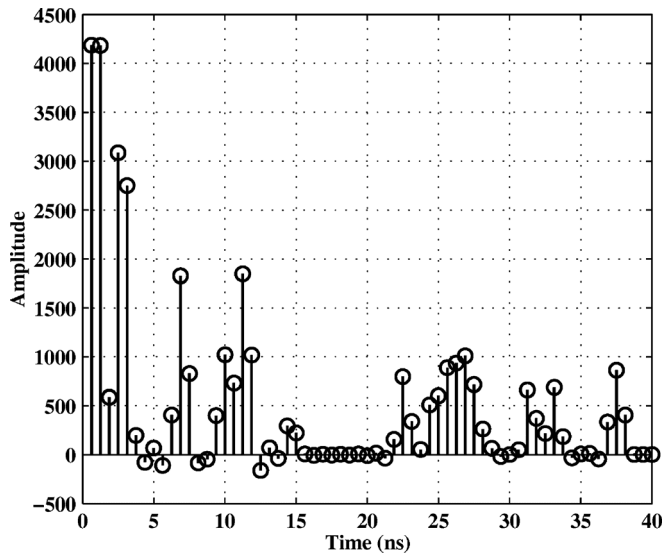

Fig. 2. Channel-impulse response $h(t)$ with $T_f = 40$ ns.

C. Received Signal Model

The first frame of the received signal corresponding to the k-th transmitted bit without noise can be expressed as

$$r_k(t) = b(k) \cdot \sum_{\ell=0}^{L-1} \alpha_\ell p(t - kT_b - \tau_\ell). \tag{3}$$

Since we assume $T_f \geq \tau_{L-1} + T_p$ and $h(t)$ is static within N_s bits, the total received signal can be written as follows:

$$r(t) = \sum_k \sum_{j=0}^{N_f-1} r_k(t - jT_f) + w(t) \tag{4}$$

where $w(t)$ is considered as an additive white Gaussian noise (AWGN) process with zero-mean.

We consider two different receiver designs, rake receivers [14] and correlator receivers [15] and compare their performances. These two methods require channel estimation as a template and we use a data-aided framework (or so-called pilots) to satisfy this. We transmit N_p known pilot bits to

estimate the channel impulse response for each packet of N_s bits. The rest of $(N_s - N_p)$ information bits are detected based on the acquired noisy channel template. In other words, the received pilot bits are within the interval $0 < t \leq T_w$, where $T_w = N_w T_f$ and $N_w = N_p N_f$ and the received information bits are during $T_w < t \leq N_s N_f T_f$. In particular, considering the received signal over the periods $jT_f \leq t < (j+1)T_f$ for $j = 0, 1, \ldots, N_w - 1$ and assuming perfect timing synchronization, the received pilot signal in one frame duration is

$$r_f^j(t) = b\left(\left\lfloor \frac{j}{N_f} \right\rfloor\right) \sum_{\ell=0}^{L-1} \alpha_\ell p(t - jT_f - \tau_\ell) + w(t). \quad (5)$$

D. Channel Estimation

In order to have good detection of the transmitted bits, it is essential to have accurate channel estimation so that we are able to collect and combine the transmitted signal energy which is spread due to the multipath channel. To be more specific, the estimation of the channel parameters α_ℓ and τ_ℓ for $\ell = 0, 1, \ldots, L-1$ are required for our receivers. In order to capture the signal characteristic and represent the signal in sparse components, we define the basis (or so-called dictionary) $\mathcal{D} = \{d_1(t), d_2(t), \ldots, d_Z(t)\}$, where $d_j(t) = p(t - (j-1)\Delta t), j = 1, 2, \ldots, Z$ with minimum step Δt. The following procedure is similar to [5], [16]. First, we project a frame-long period of the signal with a set of K waveforms $\Phi(t) = [\phi_1(t)\phi_2(t) \cdots \phi_K(t)]^T$ with amplitudes associated with randomly chosen rows of the Hadamard matrix. For example, the first waveform can be $\phi_1(t) = 1$ for $0 \leq t \leq T_f$ since the first row of the Hadamard matrix is $[11 \cdots 1]$. The second waveform can be $\phi_2(t) = 1$ for $0 \leq t \leq T_f/2$ and $\phi_2(t) = -1$ for $T_f/2 \leq t \leq T_f$ since one row of the Hadamard matrix is $[1 \cdots 1 - \cdots - 1]$. The projected received signals $\mathbf{y}_f^j = \int_0^{T_f} \Phi(t) r_f^j(t) dt = [y_f^j[1], y_f^j[2], \ldots, y_f^j[K]]^T$, $j = 1, 2, \ldots, N_w$ are averaged over N_w frames to obtain $\mathbf{y}$ and then we use the (1) matching pursuit (MP) algorithm [12] and (2) spectral projected-gradient (SPGL1) [13] algorithm to estimate the multipath channel.

Next, we outline the idea of MP. The initialization is to set $\theta_i = 0$ for $i = 1, 2, \ldots, Z$, where θ_i for $i = 1, 2, \ldots, Z$ are the estimates of amplitude of channel impulse response at time delay $i\Delta t$. Considering the projected component $\mathbf{v}_\ell = \int \Phi(t) d_\ell(t) dt, \ell \in \{1, 2, \ldots, Z\}$, the first step for the first iteration of the MP algorithm is to choose the vector which has the largest absolute value of the correlation with the received signal $\mathbf{y}$, that is $\mathbf{v}_j = \arg\max_{\mathbf{v}_\ell} |\langle \mathbf{y}, \mathbf{v}_\ell \rangle| / \|\mathbf{v}_\ell\|$. The second step is to update the corresponding coefficient and the time delay of the chosen vector: $\theta_j \leftarrow \theta_j + \langle \mathbf{y}, \mathbf{v}_j \rangle / \|\mathbf{v}_j\|^2$. Then, we subtract the selected component from the received signal: $\mathbf{y} \leftarrow \mathbf{y} - \langle \mathbf{y}, \mathbf{v}_j \rangle \mathbf{v}_j / \|\mathbf{v}_j\|^2$. The second iteration starts after the subtraction. The whole algorithm is terminated when the number of iterations reaches a preset value, say T_0 or the energy of the remaining signal is below some threshold.

After MP, the sparse vector $\Theta = [\theta_1, \theta_2, \ldots, \theta_Z]^T$ is obtained and then $\hat{h}(t) = \sum_{i=1}^{Z} \theta_i d_i(t)$ is the estimate of $h(t) * p(t)$. In the case that the vectors in the dictionary are not orthogonal to one another, the number of iterations T_0 using MP should be larger than the number of fingers L_0 so the estimated gain θ_i of the previous selected vectors $d_i(t)$, $i \in \{\text{indices of the previous selected vectors}\}$ can be revisited and updated.

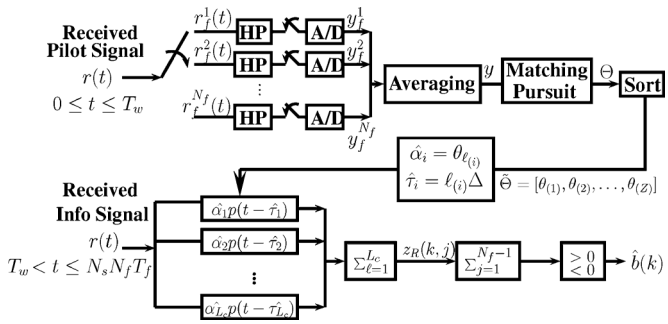

Fig. 3. CS rake receiver.

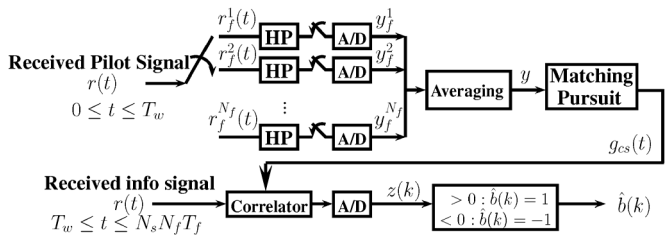

Fig. 4. CS correlator receiver.

E. CS Rake Receiver

Let $\theta_{(i)}$ for $i = 1, 2, \ldots, Z$ be the sorted element of the set $\{|\theta_1|, |\theta_2|, \ldots, |\theta_Z|\}$ and define $\theta_{(1)} = \max\{|\theta_1|, \ldots, |\theta_Z|\}$, $\theta_{(Z)} = \min\{|\theta_1|, \ldots, |\theta_Z|\}$, and $\theta_{(i_1)} \geq \theta_{(i_2)}$ for $i_1 \leq i_2$. Furthermore, define $\ell_{(i)}$ as the index in the sparse vector of the ith sorted element. The estimated path gain and path delay for the ith propagation path are

$$\begin{aligned} \hat{\alpha}_i &= \theta_{\ell_{(i)}} \\ \hat{\tau}_i &= \ell_{(i)} \Delta t \end{aligned} \quad (6)$$

for $i = 1, 2, \ldots, L_c$, where L_c is the number of paths that are considered. The received signal $r(t)$ is then correlated with a set of correlators with elements $p(t - \hat{\tau}_\ell)$ for $\ell = 1, 2, \ldots, L_c$. Then, maximum ratio combining (MRC) is applied to form a sufficient statistic to detect the kth transmitted bit in the jth frame:

$$z_R(k,j) = \sum_{\ell=1}^{L_c} \hat{\alpha}_\ell \int_{kT_b + jT_f + \hat{\tau}_\ell}^{kT_b + jT_f + \hat{\tau}_\ell + T_p} r(t) \times p(t - kT_b - jT_f - \hat{\tau}_\ell) dt. \quad (7)$$

The detection of the k bit is done by summing the statistics corresponding to the N_f frames in the same bit as follows:

$$\hat{b}(k) = \text{sgn}\left(\sum_{j=0}^{N_f - 1} z_R(k,j) \right). \quad (8)$$

The whole structure of the CS Rake-based detector is shown in Fig. 3. HP refers to the Hadamard projection in Figs. 3–6.

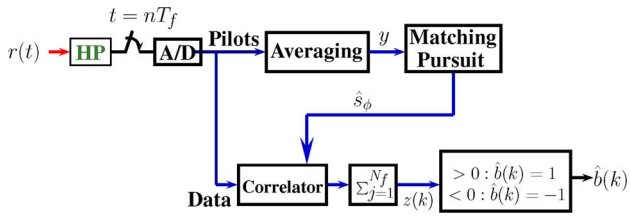

Fig. 5. CS correlator receiver with smashed filters.

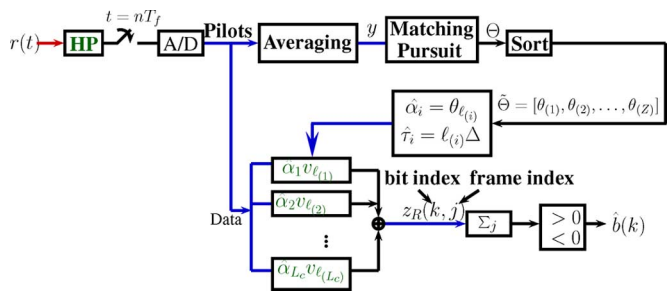

Fig. 6. CS rake receiver with smashed filters.

F. CS Correlator Receiver

The CS correlator receiver is similar to the CS rake receiver with the difference that we use $\hat{h}(t) = \sum_i \hat{\alpha}_i p(t - \hat{\tau}_i)$ as the channel template $g_{cs}(t)$. When the number of fingers in the rake receiver is the same as number of the nonzero path gain α_i, the performance of these two receiver are the same. The channel template g_{cs} is then correlated with the received information signal to perform detection at the sampling rate of one frame. The detection of the kth bit is summing the statistics corresponding to the N_f frames of the same bit as formulated below:

$$z(k) = \sum_{j=0}^{N_f - 1} \int_{jT_f + kT_b}^{(j+1)T_f + kT_b} r(t) g_{cs}(t - jT_f - kT_b) dt \qquad (9)$$

The structure of the CS correlator receiver is shown in Fig. 4.

G. CS Receivers With Smashed Filters

In [5], the estimated channel template $\hat{h}(t)$ is used to correlate with the received information bit waveforms in the analog domain, or in digital domain after being sampled at the Nyquist rate. To reduce the sampling rate and apply the same circuit processing to both the received pilot and information bits, we assume a smashed filter in our CS correlator and rake receiver, as shown in Figs. 5 and 6. The difference between these receiver structures is that the received information bits are also projected with the Hadamard transform to the compressed domain and become $\mathbf{y}$ with the same circuit used for the pilot signals and correlated with the compressed version of the channel template $\hat{\mathbf{s}}_\phi = \sum_{i=1}^{Z} \theta_i \mathbf{v}_i$ to perform bit detection.

III. Proposed Hardware

The receiver architectures considered in Section II all required that Hadamard Projections (HP) be computed of the incoming input signal and subsequently digitized by an ADC. To allow the practical implementation of these receivers, in this section we propose a hardware architecture with practical constraints for computing HPs. The goal is to propose an architecture that will not only allow us to take HPs [by computing the Walsh–Hadamard Transform (WHT)] but which is also amenable for circuit implementation in an ASIC.

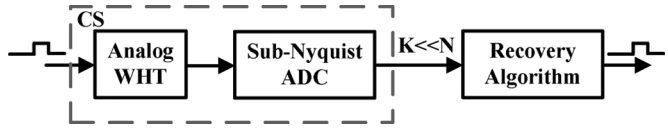

Fig. 7. Block diagram of a CS acquisition system.

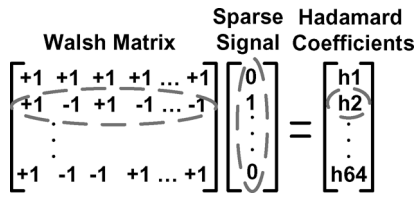

Fig. 8. Hadamard transform.

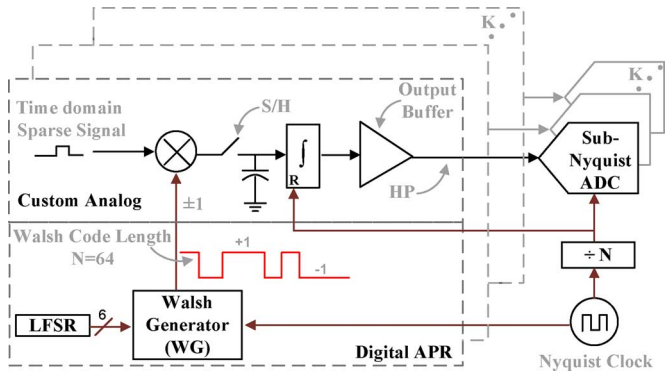

Fig. 9. Block diagram of analog WHT front-end.

Fig. 7 shows the block diagram of a hardware system exploiting the WHT as a measurement matrix in a CS system. Our signal of interest is a baseband UWB pulse which is sparse in the time domain. An analog WHT is computed on the incoming sparse signal, the output of which is sub-Nyquist sampled by randomly choosing K WHT coefficients out of N possible samples assuming a Nyquist grid. The compressed samples may then be post-processed if needed (depending on the particular receiver architecture) using a recovery algorithm (e.g., L1 minimization) which reconstructs the original sparse signal in the time domain [13], [17].

As a practical architecture exploiting CS for computing analog WHT, we propose a 64-point WHT as the measurement matrix. The Hadamard coefficients are the inner products of the input signal with the Walsh codes as shown in matrix form in Fig. 8. To compute the WHT in the analog domain, a discrete-time WHT front-end is proposed, as shown in Fig. 9. The incoming UWB signal is correlated with the Walsh codes using Nyquist rate sampling (typically in gigahertz range for UWB signal pulses) and discrete-time integration.

The detailed operation of the proposed discrete-time WHT to compute HP is as follows. A 6-bit linear feedback shift register

(LFSR) generates a pseudo-random number which is used by the Walsh code generator (WG) from [18], to generate the Walsh code of that sequency. This is equivalent to randomly selecting a row (i.e. a Walsh sequence) in the WHT matrix. The input is sampled at the Nyquist rate by the *S/H* circuits with either positive or negative polarity depending on the current value of the Walsh sequence. The circuit operates in two phases: sampling and integration. After the input is sampled with the appropriate polarity, the circuit enters into the integration phase to integrate the sampled values. At the end of the integration phase, the input signal has been correlated with the generated 64-point Walsh sequence. The integrator is reset and the computed Hadamard coefficient is then digitized by the sub-Nyquist ADC. The *S/H* circuit is sampling the input signal at the required Nyquist rate while the Hadamard coefficients are being output at every 64th sample of the input signal (since the input is correlated with a 64-point Walsh sequence).

The above process produces one Walsh coefficient. Now there are two possibilities for a CS system which requires computing K compressed coefficients. First, is the parallel architecture in which the proposed hardware is repeated K times and the K Hadamard coefficents are computed in parallel by simultaneously correlating the input with K different Walsh sequences. This will require replicating the sub-Nyquist ADC by K times or increasing the sampling rate for the sub-Nyquist ADC to be $(K/N) \times \text{the required Nyquist rate}$ (here $N = 64$). Second, is the series architecture in which the K Hadamard coefficients are computed in series. This puts a restriction on the input to be repetitive for K times to enable the Hadamard computation by correlating the input with K different Walsh sequences in series. In this case the sub-Nyquist ADC sampling rate will be $(1/N) \times \text{the required Nyquist rate}$ for the input $(N = 64)$. The proposed architecture can be adapted for either series or parallel implementation, or a combination of both.

IV. Design Decisions

Three important questions need to be addressed regarding architectural design decisions. First, how to choose the optimum number of compressed measurements (K) or compression ratio $(N - K)/N$. Second, how to choose the resolution of the sub-Nyquist ADC. Third, how the proposed CS hardware with sub-Nyquist ADC compares with using a Nyquist ADC without CS. For this purpose a Matlab simulation was setup for the architecture shown in Fig. 7 for different random measurements (K) and resolutions of the sub-Nyquist ADC. In order to investigate the effect of CS only, it is assumed in this simulation that the transmitted pulse passes through an ideal channel with no additive noise. Fig. 10 shows the mean square error (MSE) between the input and the recovered pulse (averaged for 100 iterations) as a function of the number of random measurements (K) for different resolutions of the sub-Nyquist ADC. The right y-axis marks the mean square quantization error (MSQE) for the input pulse quantized by a Nyquist ADC without CS for comparison.

It is observed that for about $K \geq N/3$ the MSE does not depend on K, but is limited by the resolution of the sub-Nyquist ADC quantizing the Hadamard coefficients. Furthermore, by comparing the recovered pulse's MSE with the MSQE of a Nyquist ADC, we observe that the sub-Nyquist ADC quantizing a signal in the Hadamard domain saves roughly one bit

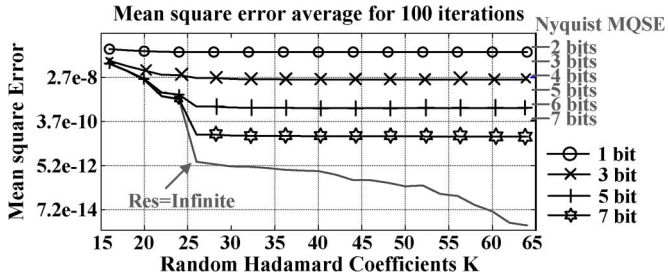

Fig. 10. MSE as a function of K.

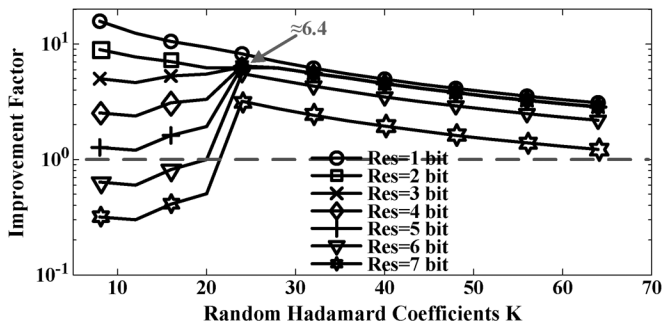

Fig. 11. Improvement factor over Nyquist ADC.

of resolution for the same quantization error as for the Nyquist ADC quantizing in the time domain.

An ADC figure-of-merit (FoM) is defined as

$$\text{FoM} = \frac{\text{Power}}{2^{\text{ENOB}} \times f_s} \tag{10}$$

where ENOB is the effective number of bits, f_s is the sampling frequency, and Power is the total power consumption of an ADC. Since an ideal ADC is assumed in this paper, in that case ENOB is equal to the resolution of the ADC. By taking compressed samples K assuming the architecture in Fig. 9, the sampling rate for the sub-Nyquist ADC reduces to $(K/N) \times f_s$. Furthermore, as mentioned above a sub-Nyquist ADC quantizing Hadamard coefficients can save one bit in resolution over a Nyquist ADC quantizing time samples. Combining these two factors, we define an Improvement Factor (IF) for the sub-Nyquist ADC as, $IF = 2^x \times N/K$ where x is the savings in ENOB and (N/K) is the reduction in the sampling rate. For the same FoM, IF is the factor by the power of the sub-Nyquist ADC is reduced relative to the Nyquist ADC. Fig. 11 shows the simulated IF as a function of K for different resolutions of the sub-Nyquist ADC. The dashed line in the plot represents $IF = 1$, below which the sub-Nyquist ADC consumes more power than the Nyquist ADC. There clearly exists an optimum value of $K = 24$ for which the IF shows a peak. At the peak value of IF, the power of a sub-Nyquist ADC can be reduced by a factor of 6. Fig. 12 shows the IF for 5 bit resolution of the sub-Nyquist ADC along with its constituent components. As expected the (N/K) factor decreases as we take more compressed measurements (K) and the resolution factor (2^x) saturates at about $K \geq N/3$, which explains the peaking effect of the IF.

Now to answer the three questions relating to the architecture implementation, the resolution of the sub-Nyquist ADC can be chosen based on the intended application requirements for the

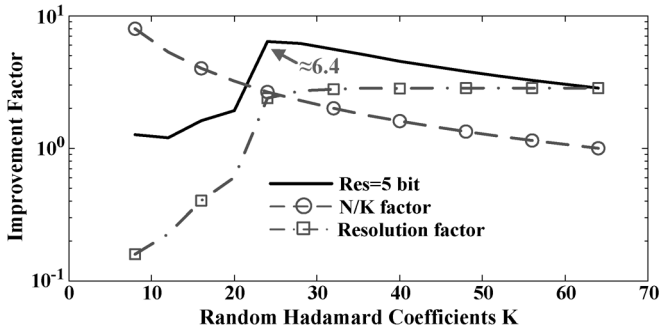

Fig. 12. Improvement factor for $\mathrm{Res} = 5$ bit.

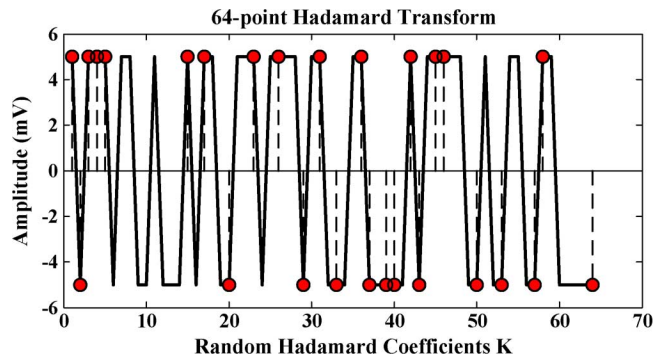

Fig. 13. Hadamard transform.

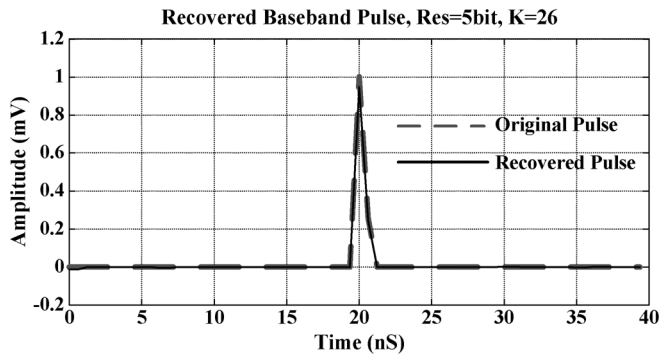

Fig. 14. Recovered pulse.

MSQE. Once the resolution of the sub-Nyquist ADC is chosen, there exists an optimum value of K for which IF is maximum. At around the peak value of IF the power of the sub-Nyquist ADC can be reduced by a factor of about 6 when compared with the Nyquist ADC.

Fig. 13 shows the 64-point Hadamard transform for an input pulse along with $K = 26$ randomly selected coefficients chosen out of $N = 64$. Fig. 14 shows the recovered pulse in the time domain using SPGL1 from [13] with a 5-bit resolution for the sub-Nyquist ADC.

The MSE shown in Fig. 10, to first order, is a performance metric for the proposed system. But for a communication system we are more interested in finding how the choice of K and resolution of the sub-Nyquist ADC affects the BER in an additive white Gaussian noise (AWGN) channel, which is investigated in the next section.

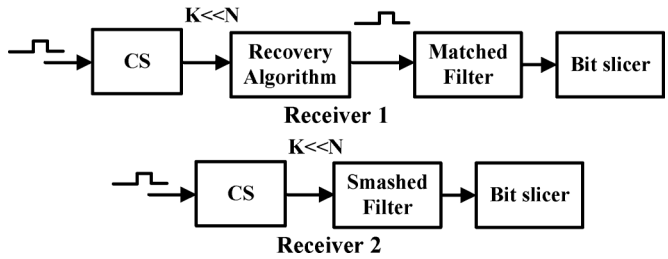

Fig. 15. Receiver architectures for waterfall curves.

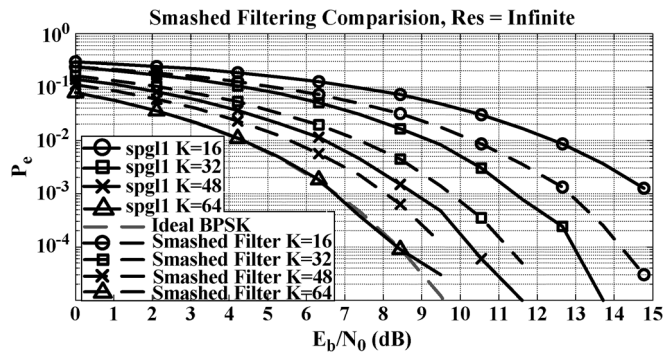

Fig. 16. BER curves for infinite resolution.

V. Simulation Results

A. Perfect Channel Estimation

To generate the waterfall curves assuming an ideal channel with AWGN noise, two different receiver architectures were considered, both based on matched filtering as shown in Fig. 15. In the first architecture, compressed samples are taken in the Hadamard domain and the time-domain sparse signal is recovered using SPGL1 which is then correlated with an ideal template to make bit decisions. In the second architecture, the difference is that matched filtering is done directly in the Hadamard domain using sub-Nyquist samples (also known as smashed filtering in the CS literature) rather than in the time domain after reconstruction.

Fig. 16 shows the bit error rate (BER) curves for both receiver architectures for infinite resolution of the sub-Nyquist ADC and compares it with an ideal BPSK curve for different values of K. It is found that the smashed filter has better performance compared to the matched filter in the time domain. One explanation for this is that the recovery algorithm attempts to find a sparse solution in the time domain to a given set of compressed measurements K. However, a signal with low SNR cannot be considered sparse, because noise produces many nonzero values. The recovery algorithm in the CS framework assumes a sparse solution to the given set of compressed measurements. As a result, the algorithm attempts to reconstruct the noise with the sparse solution. This affects the performance of the matched filter and results in an increased probability of error (Pe) at a given signal-to-noise ratio (E_b/N_0) for $K < N$. We believe that this is a strong function of the recovery algorithm being used and should be investigated further in future work.

Fig. 17 shows the BER curves for 5bit resolution of the sub-Nyquist ADC quantizing Hadamard coefficients. In this case the BER curve for $K = N = 64$ doesn't overlap the ideal

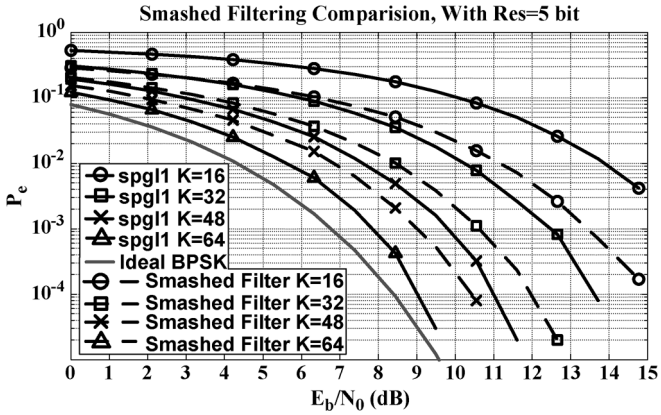

Fig. 17. BER curves for $\mathrm{Res} = 5$ bit.

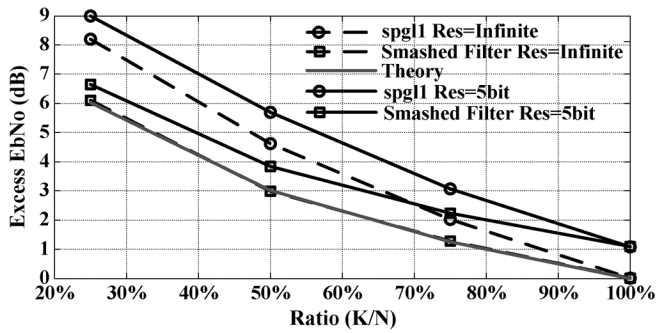

Fig. 18. Excess E_b/N_0 vs. compressions ratio for $\mathrm{BER} = 10^{-3}$.

BPSK curve due to the quantization noise. Next we define excess E_b/N_0 as the extra energy per bit required in the CS receiver in order to achieve the same BER as that of an ideal BPSK receiver. The excess E_b/N_0 required for different values of K at a BER of 10^{-3} is shown in Fig. 18. Both receiver architectures are compared along with infinite and 5bit resolution for the sub-Nyquist ADC. Using a smashed filter with 5-bit resolution requires an excess E_b/N_0 of about 1dB. The excess E_b/N_0 for the smashed filter with infinite resolution overlaps the theoretical predicted loss in SNR curve when K random Hadamard coefficents out of N samples are chosen [19]. The theoretical loss in SNR in dB is given by

$$\text{Loss in SNR(dB)} = 10\log_{10}\left(\frac{N}{K}\right). \tag{11}$$

This result is very important for a designer to consider when designing a compressed sensing system. There is inherent loss in SNR by the same factor that the compressed samples are taken (choosing K random coefficients out of total N samples results in a K/N loss in SNR).

B. Multipath Channel Estimation

In this section, we consider the case where the multipath channel impulse response is estimated by the receivers. The channel model we used is IEEE 802.15.4a standard. In the standard, all the parameter values are specified. We would like to point out that the BER performance of the receivers in Figs. 19–24 are for smashed filtering and in Figs. 25 and 26 are for matched filtering. Fig. 19–22 discussed below are with

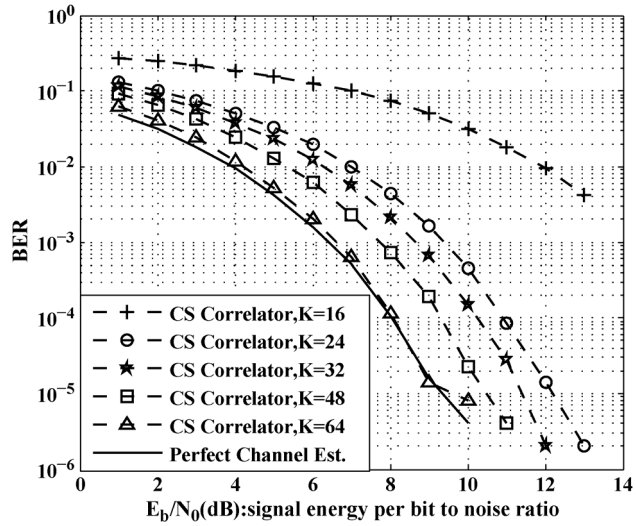

Fig. 19. BER Performance for different number of projected measurement $K = 16, 24, 32, 48, 64$, no quantization, smashed filter, SPGL1. The BER curves for CS rake and correlator are nearly identical to that of CS correlator.

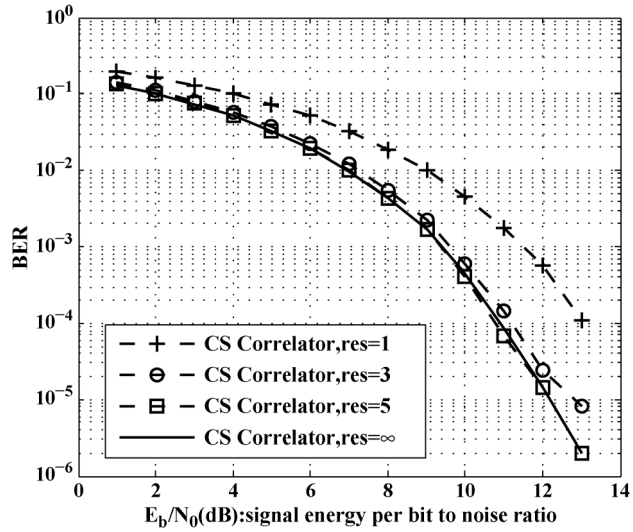

Fig. 20. BER performance for the smashed filter with different number of bit resolution: 1,3,5,∞, with $K = 24$, SPGL1. The BER curves for CS rake and correlator are nearly identical to that of CS correlator.

a fixed number of fingers $L_c = 50$ in the CS rake receiver and a fixed number of pilot bits $N_p = 128$. We first focus on smashed filtering since with perfect channel estimation it is found to be better than matched filtering. We evaluate the BER performance of the receiver without quantization for different values of K and using the smashed filter to correlate the received signal with a noisy estimated channel template in Fig. 19. The waterfall curves show that the BER performance is improved when K is increased, as expected. Fig. 20 shows the BER performance of the smashed filter for different quantization resolutions with a fixed $K = 24$. It is observed that there is 2 dB gap between 1-bit and 3-bit quantization resolution but beyond 5-bit resolution, the improvement is insignificant. This 2 dB gap conforms to the common knowledge that the performance of a hard decision detector is often $2 \sim 3$ dB worse than that of a soft decision detector. The receiver with 1-bit quantization resolution is essentially a hard decision detector

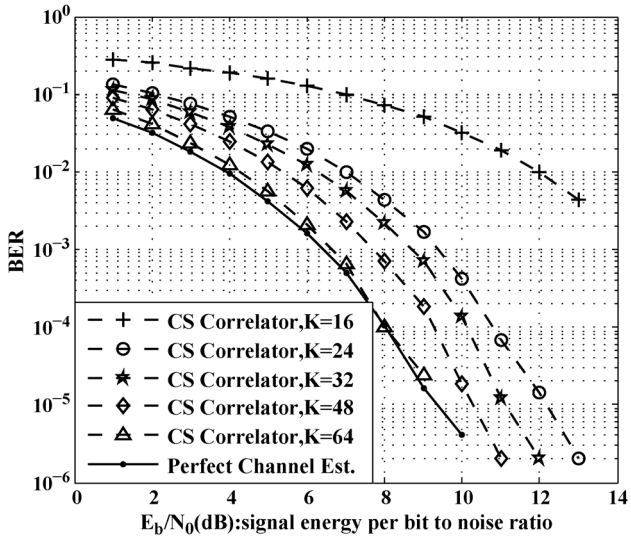

Fig. 21. BER Performance for different number of projected measurement $K = 16, 24, 32, 48, 64$, with quantization resolution $= 5$ bits, smashed filter, SPGL1. The BER curves for CS rake and correlator are nearly identical to that of CS correlator.

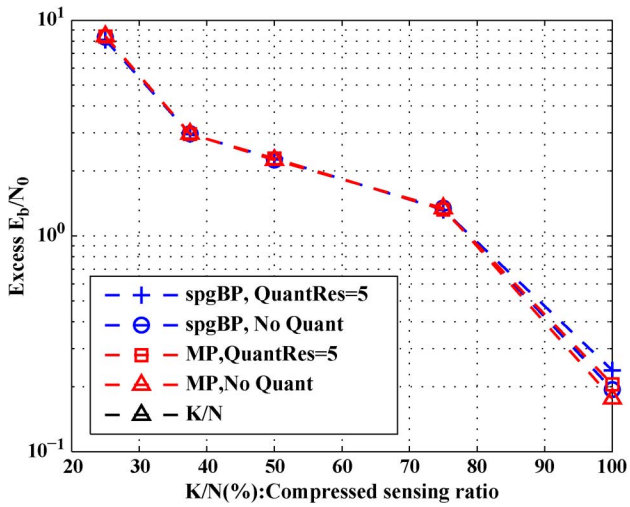

Fig. 22. Excess E_b/N_0 required for different K in different receiver schemes.

and the receiver with 7-bit quantization is very close to an ideal soft decision detector.

Hence, in Fig. 21, we fix the quantization resolution at 5 bits and vary the value of K. It shows again that the BER performance is improved through increasing the number of K, as expected.

Next, instead of using the SPGL1 algorithm to recover the channel output estimation, we use the MP algorithm to recover the multipath channel template in the receiver. The performance of MP is similar to the previous case using the SPGL1 algorithm. The larger the K used in the receiver, the better the performance we acquire.

The comparison between the receivers with SPGL1 and MP algorithm is shown in Fig. 22. This figure shows the excess E_b/N_0 needed to achieve $P_e = 10^{-3}$ versus K/N of four different receivers with quantization resolution of 5-bits or without quantization and using the MP or SPGL1 algorithm. It is interesting to notice the significant drop of excess E_b/N_0 from

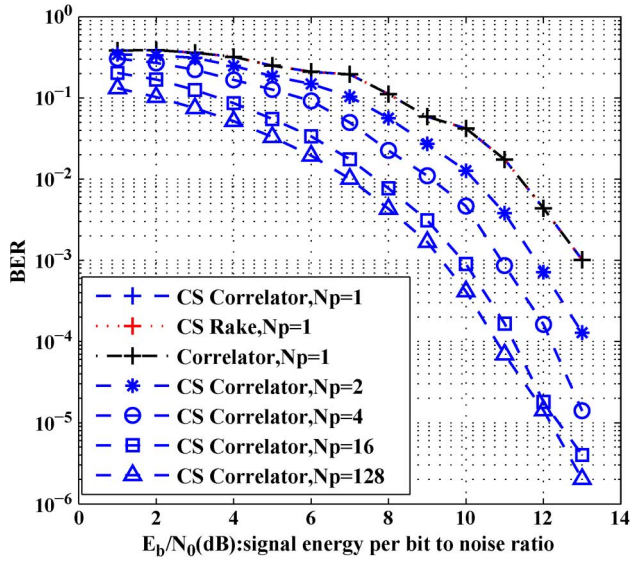

Fig. 23. BER Performance for different number of pilot bits $N_p = 1, 2, 4, 16, 128$, with $K = 24$, $L_c = 50$, smashed filter, SPGL1. The BER curves for CS rake and correlator are nearly identical to that of CS correlator.

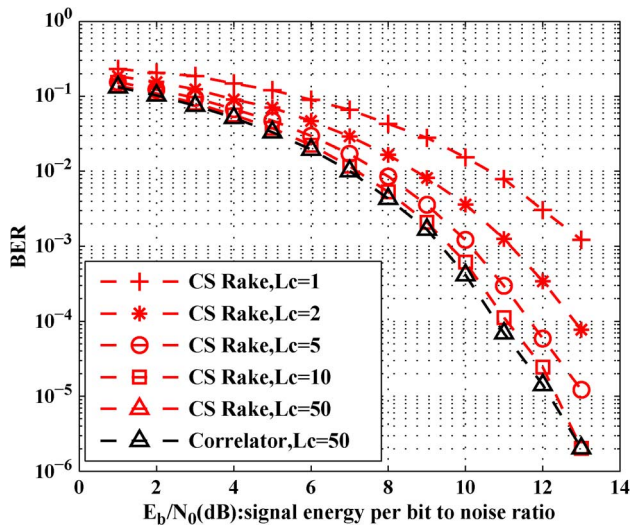

Fig. 24. BER Performance for different number of fingers in Rake receiver $L_c = 1, 2, 5, 10, 50$, $N_p = 128$, with $K = 24$, quantization resolution $= 5$ bits, smashed filter, SPGL1. The BER curves for correlator are nearly identical to that of CS correlator.

$K/N = 25\%$ $(K = 16)$ to $K/N = 37.5\%$ $(K = 24)$. We also observe that the 4 curves are nearly identical.

Fig. 23 shows the BER waterfall curves with different values of N_p and fixed $L_c = 50$. It is observed that the 3 different receiver structures (CS correlator, CS rake, and correlator) have almost the same performance for each value of N_p. For simplicity, we only show three different structures for $N_p = 1$ and for other values of N_p, we only show the curves for the CS correlator. On the other hand, Fig. 24 shows a different phenomenon that by increasing the number of fingers L_c in the Rake receiver, the performance improves for the Rake receiver while the performance of the other two receivers remains the same, as expected. We also omit the curves for the CS Correlator for simplicity.

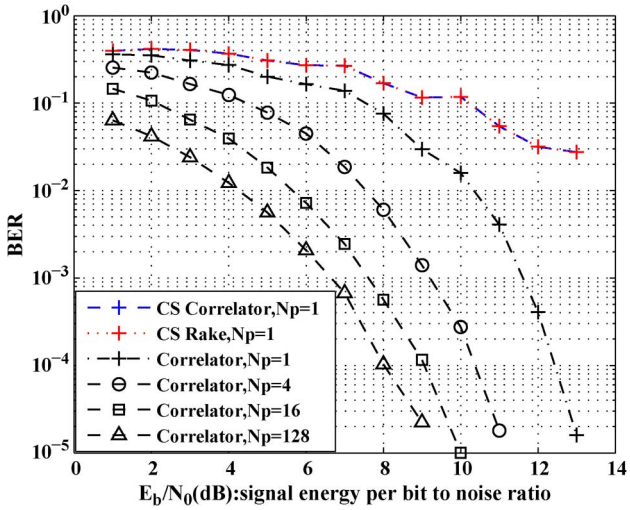

Fig. 25. BER Performance for different number of pilot bits $N_p = 1, 4, 16, 128$, with $L_c = 50$, $K = 24$, quantization resolution $= 5$ bits, SPGL1. The BER curves for CS rake are nearly identical to that of CS correlator.

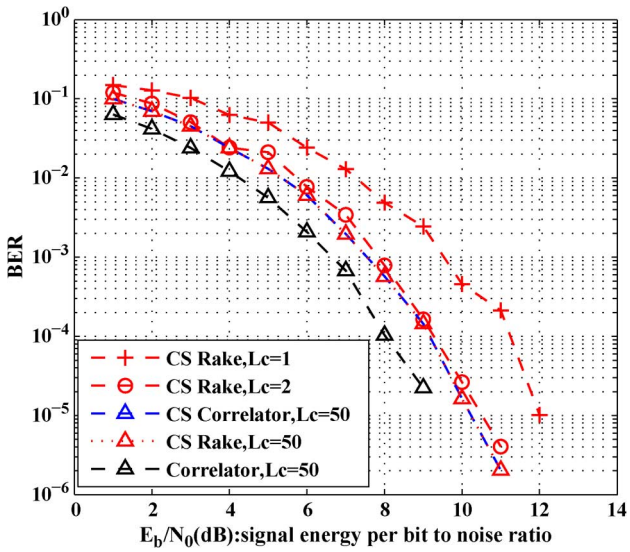

Fig. 26. BER Performance for different number of fingers $L_c = 1, 2, 5050$ in Rake receiver, with $K = 24$, quantization resolution $= 5$ bits, SPGL1.

Considering a receiver with a matched filter, Figs. 26 and 25 show the BER performance with different values of N_p while $L_c = 50$ is fixed and various values of L_c while $N_p = 128$ is fixed. Notice that the performance of $L_c = 2$ is quite close to that of $L_c = 50$, when $N_p = 128$ is fixed. On the other hand, when L_c is fixed at 50, increasing the number of pilot bits gradually improves the performance without any large jumps.

VI. Conclusion

In this paper, we use compressed sensing to reduce the sampling rate and power consumption of the proposed hardware. Circuit design parameters such as the number of compressed measurements K and the effects of quantization are investigated under the condition of perfect channel estimation. We also compared the performance of receivers using a smashed filter in the compressed domain and using a matched filter in the time domain with and without quantization. We found that quantizing the signal in the Hadamard domain saves one bit in resolution as compared to quantizing the signal in time domain for the same MSQE. We also observed that the receiver using a smashed filter requires 1 dB less excess E_b/N_0 than that using the time domain matched filter under perfect channel estimation. It is found that for CS using a smashed filter there exists a tradeoff between the BER performance of the receiver and the power savings in the sub-Nyquist ADC by reducing its sampling rate. CS can be useful in situations where the signal SNR is high. In that case the extra SNR can be traded for power savings in the sub-Nyquist ADC to maintain a target performance. At a peak value of IF, the power consumption of the sub-Nyquist ADC can be reduced by a factor of about 6. Furthermore, we consider the multipath channel circumstances and evaluate the BER performance of the receivers with different K, quantization and recovery algorithms (SPGL1 or MP) to estimate a noisy channel template. We found that BER performance is almost the same for the recovery algorithms SPGL1 or MP, without any or with 5-bit quantization. The BER performance curve with $K = 24$ has significant improvement over $K = 16$ and it is comparable to no compression with $K = 64$. We also compared the performance of different receiver design parameters, such as number of pilot bits and number of fingers in the Rake receiver. For both receiver structures, matched filter and smashed filter, 4 pilot bits is a good trade-off between BER performance and energy consumption. On the other hand, while using a matched filter, the 2-finger rake receiver has almost the same performance as the 50-finger receiver. While using a smashed filter, we need to use a 5-finger rake receiver to achieve comparable performance to the 50-finger rake receiver.

Acknowledgment

The authors would like to thank Prof. A. C. Gilbert for her valuable discussions.

References

[1] P. Scholtens and M. Vertregt, "A 6-b 1.6-gsample/s flash adc in 0.18-μm cmos using averaging termination," *IEEE J. Solid-State Circuits*, vol. 37, no. 12, pp. 1599–1609, Dec. 2002.

[2] K. Uyttenhove and M. Steyaert, "A 1.8-v 6-bit 1.3-ghz flash adc in 0.25- μm cmos," *IEEE J. Solid-State Circuits*, vol. 38, no. 7, pp. 1115–1122, July 2003.

[3] C. Sandner, M. Clara, A. Santner, T. Hartig, and F. Kuttner, "A 6-bit 1.2-gs/s low-power flash-adc in 0.13- μm digital cmos," *IEEE J. Solid-State Circuits*, vol. 40, no. 7, pp. 1499–1505, July 2005.

[4] R. Hoctor and H. Tomlinson, "Delay-hopped transmitted-reference rf communications," in *2002 IEEE Conf. on Ultra Wideband Systems and Technologies, Dig. of Papers*, 2002, pp. 265–269.

[5] J. L. Paredes, G. R. Arce, and Z. Wang, "Ultra-wideband compressed sensing: Channel estimation," *IEEE J. Sel. Topics Signal Process.*, vol. 1, no. 3, pp. 383–395, 2007.

[6] C. Berger, Z. Wang, J. Huang, and S. Zhou, "Application of compressive sensing to sparse channel estimation," *IEEE Commun. Mag.*, vol. 48, no. 11, pp. 164–174, November 2010.

[7] G. Gui, Q. Wan, W. Peng, and F. Adachi, "Sparse multipath channel estimation using compressive sampling matching pursuit algorithm," *CoRR*, vol. abs/1005.2270, 2010.

[8] G. Gui, Q. Wan, and W. Peng, "Fast compressed sensing-based sparse multipath channel estimation with smooth l0 algorithm," in *2011 3rd Int. Conf. on Commun. Mobile Comput. (CMC)*, , April 2011, pp. 242–245.

[9] D. Donoho, "Compressed sensing," *IEEE Trans. Inf. Theory*, vol. 52, no. 4, pp. 1289–1306, Apr. 2006.
[10] E. Candes and T. Tao, "Near-optimal signal recovery from random projections: Universal encoding strategies?," *IEEE Trans. Inf. Theory,*, vol. 52, no. 12, pp. 5406–5425, Dec. 2006.
[11] M. Braun, J. Elsner, and F. Jondral, "Signal detection for cognitive radios with smashed filtering," in *IEEE 69th Veh. Technol.Conf., Spring 2009*, Apr. 2009, pp. 1–5.
[12] S. Mallat and Z. Zhang, "Matching pursuits with time-frequency dictionaries," *IEEE Trans. Signal Process.*, vol. 41, no. 12, pp. 3397–3415, Dec. 1993.
[13] E. van den Berg and M. P. Friedlander, "Probing the pareto frontier for basis pursuit solutions," *SIAM J. Sci. Computing* vol. 31, no. 2, pp. 890–912, 2008 [Online]. Available: http://link.aip.org/link/?SCE/31/890
[14] V. Lottici, A. D'Andrea, and U. Mengali, "Channel estimation for ultra-wideband communications," *IEEE J. Sel. Area Commun.*, vol. 20, no. 12, pp. 1638–1645, Dec. 2002.
[15] L. Yang and G. B. Giannakis, "Ultra-wideband communications: An idea whose time has come," *IEEE Signal Process. Mag.*, vol. 21, pp. 26–54, 2004.
[16] E. J. Candes, J. K. Romberg, and T. Tao, "Stable signal recovery from incomplete and inaccurate measurements," *Comm. Pure Appl. Math.*, vol. 59, no. 8, pp. 1207–1223, Aug. 2006.
[17] E. van den Berg and M. P. Friedlander, SPGL1: A Solver for Large-Scale Sparse Reconstruction June 2007 [Online]. Available: http://www.cs.ubc.ca/labs/scl/spgl1
[18] R. Kitai and K.-H. Siemens, "A hazard-free walsh-function generator," *IEEE Trans. Instrum. Meas.*, vol. IM-21, no. 1, pp. 80–83, Feb. 1972.
[19] M. A. Davenport, M. F. Duarte, M. B. Wakin, J. N. Laska, D. Takhar, K. F. Kelly, and R. G. Baraniuk, "The smashed filter for compressive classification and target recognition," in *Proc. SPIE*, Jan. 2007, vol. 6498, p. 64980H [Online]. Available: http://scholarship.rice.edu/jsp/handle/1911/21679

Osama Ullah Khan (S'08) received the B.E degree (with highest hons.) in electronic engineering from NED University of Engineering & Technology, Karachi, Pakistan, in 2007, and the M.S. degree in electrical engineering from University of Michigan, Ann Arbor, in 2010, and is currently pursuing the Ph.D. degree at the same university.

He has worked as an assistant manager (technical) in the Satellite Research & Development Center (SRDC), Karachi, Pakistan, from January 2007 to August 2008. In the summer of 2010, he held an internship position in the RF hardware group at Qualcomm Inc., San Diego, CA. His research interest is in Analog/RF mixed signal circuit design.

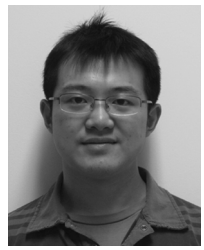

Shao-Yuan Chen (S'06) received the B.S. degree in electrical engineering from National Tsing Hua University, Hsinchu, Taiwan, in 2006 and his M.S in electrical engineering from University of Michigan, Ann Arbor, in 2011, and is currently pursuing the Ph.D. degree at the same university.

He currently also works as a research assistant in electrical engineering in University of Michigan. His research interest is focused on channel estimation in UWB system.

David D. Wentzloff received the B.S.E. degree in electrical engineering from the University of Michigan, Ann Arbor, in 1999, and the S.M. and Ph.D. degrees from the Massachusetts Institute of Technology, Cambridge, in 2002 and 2007, respectively. In the summer of 2004, he worked in the Portland Technology Development group at Intel in Hillsboro, OR. Since August, 2007 he has been with the University of Michigan, Ann Arbor, where he is currently an Assistant Professor of Electrical Engineering and Computer Science.

He is the recipient of the 2002 MIT Masterworks Award, 2004 Analog Devices Distinguished Scholar Award, 2009 DARPA Young Faculty Award, the 2009–2010 Eta Kappa Nu Professor of the Year Award, and the 2011 DAC/ISSCC Student Design Contest Award. He has served on the technical program committee for ICUWB 2008–2010 and ISLPED 2011–2012, and as a guest editor for the IEEE Transactions on Microwave Theory and Techniques, the IEEE Communications Magazine, and the Elsevier Journal of Signal Processing: Image Communication. He is a member of IEEE, IEEE Circuits and Systems Society, IEEE Microwave Theory and Techniques Society, IEEE Solid-State Circuits Society, and Tau Beta Pi.

Wayne E. Stark (S'77–M'78–SM'94–F'98) received the B.S. (with highest hons.), M.S., and Ph.D. degrees in electrical engineering from the University of Illinois, Urbana, in 1978, 1979, and 1982, respectively.

Since September 1982, he has been a faculty member in the Department of Electrical Engineering and Computer Science at the University of Michigan, Ann Arbor where he is currently Professor.

From 1984 to 1989, Dr. Stark was Editor for Communication Theory of the IEEE TRANSACTIONS ON COMMUNICATIONS in the area of Spread-Spectrum Communications. He was involved in the planning and organization of the 1986 International Symposium on Information Theory, held in Ann Arbor, MI. He was selected by the National Science Foundation as a 1985 Presidential Young Investigator. He was principal investigator of a Army Research Office Multidisciplinary University Research Initiative (MURI) project on Low Energy Mobile Communications. He received the IEEE Milcom Board 2002 Technical Achievement Award for sustained contributions to military communications. He received the IEEE Milcom Ellersick prize as the best paper in the Unclassified Technical Program in 2009. He received the best paper award from the *Journal on Communications and Networks* in 2010. His research interests are in the areas of wireless communication theory and wireless networks.